

NACA RM A52A14

0133339

TECH LIBRARY KAFB, NM

NACA

## RESEARCH MEMORANDUM

THEORETICAL INVESTIGATION OF THE STABILITY AT NEGATIVE  
 STATIC MARGINS OF A SUPERSONIC MISSILE WITH AN  
 AUTOPILOT SENSITIVE TO PITCH ANGLE  
 AND PITCHING VELOCITY

By Henry A. Cole, Jr., and Marvin Abramovitz

Ames Aeronautical Laboratory  
 Moffett Field, Calif.

Classified

By

Nasa Tech Pub Announcement #112  
 (NO CHANGE)

By

11 Mar 57  
 (NO CHANGE)

PERMANENT  
 RECORD

GRADE OF OFFICER (MARKING CHANGE)

4 Apr 61

DATE

NATIONAL ADVISORY COMMITTEE  
 FOR AERONAUTICS

WASHINGTON

March 17, 1952

319.98/13



## NATIONAL ADVISORY COMMITTEE FOR AERONAUTICS

RESEARCH MEMORANDUMTHEORETICAL INVESTIGATION OF THE STABILITY AT NEGATIVE  
STATIC MARGINS OF A SUPERSONIC MISSILE WITH AN  
AUTOPILOT SENSITIVE TO PITCH ANGLE  
AND PITCHING VELOCITY

By Henry A. Cole, Jr., and Marvin Abramovitz

## SUMMARY

Stability charts covering a range of small positive and negative static margins are presented for a supersonic missile with an autopilot sensitive to angle of pitch and rate of pitch. This dynamic system is first considered in its most simplified form with a perfect control servo and separate feedback signals. Thus the effect of each type of feedback is determined. Then a simple time lag is added to the control servo, and finally the complete system is considered with a second-order control servo and a rate gyro with a simple time lag. The results in the form of stability boundaries and lines of constant damping ratio and period show that time lags have an adverse effect on stability at negative static margins, but that this can be counteracted by using ample gain in the rate-of-pitch feedback loop.

Methods of simplifying the characteristic stability equation are discussed. The assumption of two degrees of freedom in the airframe transfer function is justified by showing that the effects of other system modes on the transient response are negligible compared to effects of the short-period oscillatory system mode.

## INTRODUCTION

In order to improve the performance of a missile, satisfactory stability at small positive or even negative static margins is often necessary. For example, in long-range tailless missiles, a significant increase in maximum lift-drag ratio can be obtained by designing the wing for a negative static margin. Furthermore, some air-to-air, boost-glide missiles incur such a large shift in the center of gravity due to

fuel consumption that, in order to provide sufficient maneuverability after boost, the missile must be flown with a negative static margin in the launching phase. Since this requires automatic stabilization which is a very broad field in itself, a practical approach to the general solution is to investigate a particular example in order to obtain information which might apply to the general case.

This report presents a theoretical investigation of the stability of a variable-incidence boost-glide supersonic missile with a simple conventional autopilot over a range of airframe static margins with particular emphasis on the negative range. The effects of pitch-angle feedback, rate-of-pitch-angle feedback, autopilot gearing, and control-servo and rate-gyro dynamic characteristics on the existence and degree of stability are considered. These particular feedback signals were selected because they are characteristic of the two basic types of signals needed to stabilize a statically unstable missile, namely a positive spring-force signal and a damping-force signal. A rate-of-pitch signal is ordinarily used in missile stabilization systems for damping, and pitch angle is one of several possible signals available for providing a spring force.

A number of analytical techniques are available for an investigation of this type. (See reference 1.) Of these methods, the charts of constant damping ratio and period of the missile-autopilot principal mode plotted in the autopilot-gearing-static-margin plane appear to offer the most comprehensive representation of stability for they show not only the regions of stability but also the degree of stability. There are a number of complications, not considered in this report, which arise in an actual missile firing. For example, even though a boost-glide missile is dynamically stable, the dispersion at burn-out might be too large because of out-of-trim moments, rough air, or initial launching conditions. Furthermore, the limits of control-surface deflection and saturation of autopilot elements may introduce nonlinearities into the equations of motion. Although these complications are beyond the scope of this report, this analysis does indicate the practicability of successfully flying a statically unstable boost-glide missile with an autopilot. Furthermore, although the results are for a particular configuration, the assumptions verified in the analysis may be useful in analyzing similar problems and the conclusions may apply qualitatively to other missiles.

#### SYMBOLS

$C_m$  pitching-moment coefficient

$D$  differential operator  $\left( \frac{d}{dt} \right)$

K gearing or gain

$K_y$  radius of gyration of missile about principal lateral axis, feet

P missile-autopilot period  $\left( \frac{2\pi}{\omega \sqrt{1-\zeta^2}} \right)$ , seconds

R ratio of rate-gyro gain to displacement-gyro gain, seconds

S exposed wing area, square feet

T rate-gyro time lag, seconds

V velocity, feet per second

a body radius, feet

b wing span, feet

c wing chord, feet

$\bar{c}$  wing mean aerodynamic chord  $\left( \frac{\int_a^{b/2} c^2 dy}{\int_a^{b/2} c dy} \right)$

j  $\sqrt{-1}$

m mass, slugs


u longitudinal perturbation velocity  $\left( \frac{\Delta V}{V} \right)$

v voltage

$\chi$   $\frac{\text{force along longitudinal axis}}{\rho V^2 S}$

x distance from neutral point to center of gravity, positive when center of gravity is ahead of neutral point, feet


$\frac{x}{c}$  static margin



$z$	$\frac{\text{force perpendicular to longitudinal axis}}{\rho V^2 S}$
$\alpha$	angle of attack, radians
$\delta$	control deflection, radians
$\theta$	pitch angle, radians
$\rho$	mass density of air, slugs per cubic foot
$\tau$	$\left(\frac{m}{\rho S V}\right)$ , seconds
$\omega$	missile-autopilot natural frequency, radians per second
$\omega_s$	control-servo natural frequency, radians per second
$\zeta$	missile-autopilot damping ratio, nondimensional
$\zeta_s$	control-servo damping ratio, nondimensional

## Subscripts

$d$	displacement gyro
$e$	actuating signal
$i$	input
$o$	output
$r$	rate gyro
$s$	control servo
$u$	$\frac{\partial}{\partial u}$
$\alpha$	$\frac{\partial}{\partial \alpha}$



$$\theta \quad \frac{\partial}{\partial \theta}$$

$$\delta \quad \frac{\partial}{\partial \delta}$$

$$\dot{\alpha} \quad \frac{\partial}{\partial \left( \frac{\partial \alpha}{\partial t} \right)}$$

$$\dot{\theta} \quad \frac{\partial}{\partial \left( \frac{\partial \theta}{\partial t} \right)}$$

### ANALYSIS

The missile-autopilot system in this analysis is represented by the block diagram of figure 1. The autopilot consists of a displacement gyro, a rate gyro, a control servo, and a differential, or their equivalents. Following is a development of the transfer functions of the components and the closed-loop transfer function of the complete system, and the method of constructing period and damping-ratio curves.

#### Transfer Functions of Components

Airframe.— The missile, shown in figure 2, is a variable-incidence cruciform configuration and is assumed to be completely roll stabilized. The longitudinal equations of motion as given in reference 2 are

$$\left. \begin{aligned} (X_u + \tau D)u + X_\alpha \alpha + X_\theta \theta_o &= 0 \\ z_u u + (z_\alpha + \tau D)\alpha + (z_\theta - \tau D)\theta_o &= -z_\delta \delta \\ C_{m_u} u + (C_{m_\alpha} + C_{m_\alpha} D)\alpha + \left( C_{m_\theta} D - \frac{2\tau K_y^2}{V\bar{c}} D^2 \right) \theta_o &= -C_{m_\delta} \delta \end{aligned} \right\} \quad (1)$$

Because preliminary calculations indicated that the degree of freedom along the longitudinal axis had little effect on the stability boundaries, two degrees of freedom were assumed in deriving the

aerodynamic transfer function. If terms involving changes in forward velocity are neglected, the equations of motion become

$$\left. \begin{aligned} (z_{\alpha} + \tau D)\alpha + (z_{\theta} - \tau D)\theta_o &= -z_{\delta}\delta \\ (C_{m_{\alpha}} + C_{m_{\alpha}}D)\alpha + \left(C_{m_{\theta}}D - \frac{2\tau K_y^2}{V\bar{c}} D^2\right)\theta_o &= -C_{m_{\delta}}\delta \end{aligned} \right\} \quad (2)$$

If the equations are solved for  $\theta_o/\delta$ , the airframe transfer function may be easily derived giving:

$$\frac{\theta_o}{\delta} = \frac{a_1 D + b_1}{D(a_2 D^2 + b_2 D + c_2)} \quad (3)$$

where

$$a_1 = z_{\delta} C_{m_{\alpha}} - \tau C_{m_{\delta}}$$

$$b_1 = z_{\delta} C_{m_{\alpha}} - z_{\alpha} C_{m_{\delta}}$$

$$a_2 = -\frac{2\tau^2 K_y^2}{V\bar{c}}$$

$$b_2 = \tau(C_{m_{\theta}} + C_{m_{\alpha}}) + \frac{a_2}{\tau} z_{\alpha}$$

$$c_2 = \tau C_{m_{\alpha}} + z_{\alpha} C_{m_{\theta}}$$

The stability derivatives for the missile were calculated from wind-tunnel data for a Mach number of 2.0 and a pressure altitude of 30,000 feet. All the derivatives including the ones required in the three-degrees-of-freedom transfer function of reference 2 are listed as functions of static margin in table I. As usual small angles were assumed.

Autopilot.— The displacement gyro is assumed to be perfect with a voltage output proportional to pitch angle. Hence the transfer function is:

$$\frac{v_d}{\theta_o} = K_d \quad (4)$$

The rate gyro has a voltage output proportional to rate of pitch amplified by the gain constant  $R K_d$ . Practical experience indicates that the voltage output of the rate gyro lags the rate of pitch, and that the lag may be closely approximated by introducing the time-lag term  $T$ . This time lag, not to be confused with delay, or "dead," time, represents an exponential rise in the transient response and is sometimes called the time constant. A typical value of time lag is 0.02 second, which in the form  $1/(1 + TD)$  has approximately the same frequency response up to a frequency of 30 radians per second as a second-order dynamical system with a damping ratio of 0.7, and a natural frequency of 60 radians per second. The transfer function is:

$$\frac{v_r}{\theta} = \frac{R K_d D}{1 + TD} \quad (5)$$

The control servo responds to actuating signal as a second-order dynamical system and produces a control deflection amplified by the control-servo gearing  $K_s$ . Hence:

$$\frac{\delta}{v_e} = \frac{K_s}{1 + \frac{2\zeta_s}{\omega_s} D + \frac{1}{\omega_s^2} D^2} \quad (6)$$

The term  $2\zeta_s/\omega_s$  has the dimensions of time and may be considered to be a time lag in the same sense as  $T$  when the frequency is high enough to make the second-order term insignificant.

Airframe and autopilot combination.— By the algebra of block diagrams in closed loops described in reference 3, the closed-loop transfer function of the missile with autopilot (fig. 1) is obtained.

$$\frac{\theta_o}{\theta_i} = \frac{K_s K_d (a_1 D + b_1) (1 + TD)}{\left(1 + \frac{2\zeta_s}{\omega_s} D + \frac{1}{\omega_s^2} D^2\right) D (a_2 D^2 + b_2 D + c_2) (1 + TD) + K_d K_s [1 + (R + T) D] (a_1 D + b_1)} \quad (7)$$

The denominator of this transfer function determines the stability of the missile-autopilot combination and, when set equal to zero, is known as the characteristic stability equation. When the aerodynamic coefficients  $a_1$ ,  $b_1$ ,  $b_2$ , and  $c_2$  are expressed in terms of  $x/\bar{c}$ , the coefficients of the characteristic equation above are functions only of  $a_2$ ,  $x/\bar{c}$ ,  $K_d K_s$ ,  $R$ ,  $T$ ,  $\zeta_s$ , and  $\omega_s$ .

Of these variables  $T$  and  $\omega_s$  are more or less determined by physical limitations of existing equipment, and  $a_2$  is fixed by the inertial characteristics of the airframe which are assumed constant in



the example. Hence,  $x/\bar{c}$ ,  $K_d K_s$ ,  $\xi_s$ , and  $R$  are the principal variables. For purposes of comparison with the time constants  $\xi_s$  is considered in the form  $2\xi_s/\omega_s$ .

#### Method of Constructing Period and Damping-Ratio Curves

Curves of constant period and damping ratio were determined by the method of reference 4 and by solution of the roots of the characteristic stability equation. The former method was used to obtain the curves for the principal oscillatory mode and the latter method to obtain the curves for all modes of motion. The Hurwitz-Routh criteria was applied where practical as a check (reference 1).

In applying the method of reference 4 to obtain curves of constant period and damping ratio in the autopilot-gearing-static-margin plane, the simultaneous equations from the real and imaginary parts were simplified in a manner depending on the frequency range. For example, in determining the stability boundary ( $\xi = 0$ ),  $D = j\omega$  is substituted in the characteristic stability equation. Separating real and imaginary parts and solving each for  $K_d K_s$  gives:

$$K_d K_s = \frac{-\frac{a_2}{\omega_s^2} \omega^4 + \left[ \frac{c_2}{\omega_s^2} + b_2 \left( \frac{2\xi_s}{\omega_s} + T \right) + a_2 \right] \omega^2 - c_2 + T \left[ -\left( a_2 \frac{2\xi_s}{\omega_s} + \frac{b_2}{\omega_s^2} \right) \omega^4 + c_2 \frac{2\xi_s}{\omega_s} \omega^2 \right]}{a_1 + b_1 (R + T)}$$

from the imaginary part and

$$K_d K_s = \frac{-\left[ \frac{b_2}{\omega_s^2} + a_2 \left( \frac{2\xi_s}{\omega_s} + T \right) \right] \omega^4 + \left[ c_2 \left( \frac{2\xi_s}{\omega_s} + T \right) + b_2 \right] \omega^2 + T \left[ \frac{a_2}{\omega_s^2} \omega^6 - \left( b_2 \frac{2\xi_s}{\omega_s} + \frac{c_2}{\omega_s^2} \right) \omega^4 \right]}{-a_1 (R + T) \omega^2 + b_1}$$

from the real part.

If  $K_d K_s$  from real and imaginary parts are equated, a cubic equation in  $\omega^2$  results, but, if order of magnitude of terms is considered, this may be reduced to a quadratic as follows: For high values of  $\omega^2$ ,  $b_1$  may be neglected in the denominator of  $K_d K_s$  from the real part because  $-a_1(R+T)\omega^2 \gg b_1$ . Except at high frequencies where the  $\omega^6$  term becomes important, the last terms in the numerators of both expressions of  $K_d K_s$  may be neglected because the coefficients involve products of two of the small quantities  $T$ ,  $1/\omega_s^2$  and  $2\xi_s/\omega_s$ .

Furthermore, terms in  $1/\omega_s^2$  may be neglected if  $\omega_s$  is large enough so that  $1/\omega_s^2 \ll \left(\frac{2\zeta_s}{\omega_s} + T\right)$  and  $\omega \ll \omega_s$ . This corresponds to the assumption of a first-order servo. In the example which follows the low-frequency assumption was found valid for determining the lower boundary and the high-frequency assumption for the upper boundary. These simplifications also apply to the equations for determining curves of constant damping ratio. These curves were obtained by substituting  $D = -\zeta\omega + j\omega\sqrt{1-\zeta^2}$  in the characteristic stability equation.

From the values of frequency and damping ratio obtained above, the period was determined and cross plotted with  $x/\bar{c}$  and  $K_d K_s$  to obtain curves of constant period.

It should be pointed out that this simplifying procedure only determines the stability boundaries of two oscillatory modes. To insure complete stability within these boundaries, the stability of the other modes must also be verified.

## RESULTS AND DISCUSSION

### Stability of Missile Without Autopilot

In order to determine clearly the effects of the autopilot, the stability of the missile alone is first considered. In this case autopilot gearing is zero and stability is dependent on the characteristic stability function given by the denominator of the aerodynamic transfer function  $\theta_o/\delta$ . For positive static margins, the characteristic equation has two complex conjugate roots with negative real parts which gives a convergent oscillatory motion in the transient response. As static margin is decreased,  $c_2$  goes to zero, which indicates neutral stability. This occurs at a small negative value of static margin ( $x/\bar{c} = -0.0037$ ) which is called the maneuvering point. At more negative values of static margin,  $c_2$  is negative and the characteristic stability equation has a negative real root and a positive real root which gives a nonoscillatory divergent motion.

### Stability of Simplified Cases of Missile-Autopilot Combination

When the complete missile-autopilot system of figure 1 is considered, there are so many variables that it is difficult to obtain a clear picture of the individual effects unless simplifications are made. In this

direction, before considering the complete system with all variables, the components were simplified and the stability was investigated first with displacement feedback only and then with rate feedback only. Then for each case the effect of a simple servo time lag was investigated. The stability boundaries of these cases are shown in figure 3 and are described below.

Displacement feedback only and a perfect servo

( $R = 2\zeta_s/\omega_s = 1/\omega_s^2 = 0$ ).-- In this case the stability boundary extends without limit into the negative static-margin region. As static margin becomes more negative, the autopilot gearing necessary for stability increases at a lower rate because control-moment effectiveness ( $C_{m\delta}$ ) and aerodynamic damping ( $C_{m\dot{\alpha}} + C_{m\dot{\beta}}$ ) are increasing. The damping trend would be characteristic of most aerodynamic configurations while the control-moment effectiveness would not. Hence, the variance of the shape of this boundary depends largely on the type and position of the control surface.

Displacement feedback only and a servo with a simple time lag

( $R = 1/\omega_s^2 = 0$ ,  $2\zeta_s/\omega_s = 0.02$ ).-- In this case stability is obtained only in a small region of the negative static-margin-autopilot-gearing plane. Hence, the boundary for displacement feedback only is extremely sensitive to time lags. The time lag used in this case is the same as that mentioned for the rate gyro in the analysis and is a practical value for a servo with a natural frequency of 60 radians per second.

Rate feedback only and a perfect servo ( $R=1$ ,  $2\zeta_s/\omega_s = 1/\omega_s^2 = T=0$ ).--

The characteristic equation becomes:

$$(1+TD) (D) (a_2 D^2 + b_2 D + c_2) + K_d K_s R (a_1 D + b_1) = 0$$

In this case the boundary also extends without limit into the negative static-margin region. No frequencies are noted on this boundary because the roots of the characteristic equation are always real for negative static margin, which means that the motion is nonoscillatory convergent on the stable side and nonoscillatory divergent on the unstable side. The characteristic equation also has a zero root which indicates that the system is neutrally stable with respect to pitch angle  $\theta$ . In other words the steady-state pitch angle will differ from the input pitch angle by an amount depending on the input.

Rate feedback only and a perfect servo with a simple time lag

( $R = 1$ ,  $2\zeta_s/\omega_s = 0.02$ ,  $T = 1/\omega_s^2 = 0$ ).-- This boundary is nearly identical to the one without time lag and for this reason the two curves are

shown as one. The characteristic equation is the same whether the time lag occurs in the control servo or the rate gyro. Hence, the stability boundary of a rate-feedback system is not appreciably changed by a small time lag in the control servo or the rate gyro.

### Discussion of the Simplified Cases

The results of these simplified cases indicate that neither a displacement-feedback nor a rate-feedback autopilot would give satisfactory stability at negative static margins for this configuration. In the former case, a perfect displacement signal would provide stability, but such a system is very sensitive to time lags and appears unsatisfactory for time lags of the order of those that might exist in a physical system. For the rate-feedback system, time lags of practical magnitude (0.02 second) had little effect, but this system is only neutrally stable with respect to pitch angle. Consequently, during the boost phase when the radar-guidance system is inoperative, an attitude or space reference would be necessary to insure sufficiently small dispersion at burn-out. Such a reference is provided by angle-of-pitch feedback in the complete autopilot.

### Effect of Autopilot Characteristics on Stability Boundaries

Although the simplified cases give indications of the effects of individual feedback signals, the exact effects must be determined with the complete system. In order to do this, one variable was changed while the others were held constant at a practical value. In this way, the effects of rate feedback, servo time lag, and servo natural frequency on the stability boundaries were examined and the results are shown in figures 4, 5, and 6, respectively, as described below.

Effect of rate feedback on stability boundary.- In figure 4, practical values were selected for the rate-gyro time lag, servo time lag, and servo natural frequency ( $T = 0.02$ ,  $2\zeta_s/\omega_s = 0.03$ ,  $\omega_s = 60$ ). This value of the time constant  $2\zeta_s/\omega_s$  corresponds to a damping-ratio setting of 0.9 in the control servo. In practice this would be considered a high setting for the damping ratio of a servo, but, as will be shown presently, lower settings of damping ratio give a wider range of stability. It is unlikely that higher values of servo damping ratio would be used in practice. Then various values were assigned to the rate-displacement ratio. For zero rate feedback  $R = 0$  and even for  $R = 0.02$ , the stability boundary extends only slightly into the negative region. However, if sufficient rate is used to counteract the

effect of servo time lag ( $R = 2\zeta_s/\omega_s = 0.03$ ), the boundary extends far into the negative static-margin region. Increasing rate feedback even more,  $R = 0.08$  extends the boundary even farther into the negative region. It should be noted at this point that at the higher rate there are two distinct boundaries, a lower boundary with a frequency of the order of the airframe short period and an upper boundary with a much higher frequency. If the second-order term in the control servo is neglected, this upper boundary occurs at infinity. This boundary, then, is largely dependent on the control-servo natural frequency and is more fully explained in the discussion of the effects of control-servo natural frequency.

There is no theoretical limit to the extension of the lower boundary into the negative static-margin plane by increasing rate feedback, but there are practical limitations to the amplification of the rate signal, for, if rate ratio  $R$  is increased beyond a value of 0.08, the upper boundary is lowered and the autopilot gearings required to remain in the stable region become very small. For example, at a rate ratio of 1 and a static margin of -0.04, the autopilot gearing required for stability must fall between 0.04 and 0.09. Hence, the practical limit to amplification of the rate signal depends on the minimum practical value of autopilot gearing. Furthermore, a wide range of autopilot gearings in the stable range is desirable to compensate for variations in aerodynamic

gearing  $\left(\frac{\delta_0}{\delta}\right)_{\omega=0}$  with Mach number and altitude. From this standpoint, the optimum rate is approximately 0.08 which at a static margin of -0.04 gives a range of autopilot gearings of 0.11 to 1.28.

Effect of control-servo time lag on stability boundaries.— In figure 5, the values of rate-gyro time lag ( $T = 0.02$ ) and control-servo natural frequency ( $\omega_s = 60$ ) from figure 4 were used. However, in this figure rate-displacement ratio is held constant at 0.03 and control-servo time lag is varied. For a control-servo time lag equal to the rate-displacement ratio, ( $2\zeta_s/\omega_s = R = 0.03$ ), the boundary extends well into the negative static-margin region. If servo time lag is decreased ( $2\zeta_s/\omega_s = 0.02$  which corresponds to a damping ratio of 0.6), the range of stability is greatly increased. On the other hand, if servo time lag is increased only slightly  $2\zeta_s/\omega_s = 0.04$ , the boundary curves back at a small negative value of static margin. Thus it appears that stability cannot be obtained over a wide range of negative static margins unless the time lag in the control servo ( $2\zeta_s/\omega_s$ ) is less than or equal to the rate-displacement ratio  $R$ . The reason for this is apparent, for the time lag in the control servo causes a phase lag of output to input which, for a statically unstable airframe, results in instability unless the feedback signal has a sufficient phase lead to counteract the phase lag of the servo. Since the phase lead of the combined feedback signals is dependent almost entirely on the rate ratio, stability is obtained

when the rate ratio, which is equivalent to a time lead, is set equal to the control-servo time lag. However, the phase lead of the combined feedback signals is also dependent on frequency and rate-gyro time lag, but their effects are negligible when the product of the rate-gyro time lag and the system frequency is much less than 1 ( $T_w \ll 1$ ), as is the case in the example.

Similar results are obtained when the rate ratio is higher ( $R = 0.08$ ), but the damping ratios necessary to make the time constant ( $2\zeta_s/\omega_s$ ) equal to the rate ratio are completely unrealistic ( $\zeta_s = 2.4$ ). However, since the rate ratio of 0.08 gives the widest range of stability at negative static margins, this value of rate will be used in the following discussion on the effects of control-servo frequency.

Effect of control-servo natural frequency on the stability boundary.- Inasmuch as present-day servo natural frequencies ordinarily fall between 30 and 180 radians per second, an investigation of the effect of servo natural frequency on the stability boundaries was made and the results are shown by figure 6. In this case, rate-feedback ratio, servo time lag, and rate-gyro time lag were held constant ( $R = 0.08$ ,  $2\zeta_s/\omega_s = 0.03$ ,  $T = 0.02$ ) while servo natural frequency was varied. These curves are made up of two distinct branches, as indicated by the double value of frequency at the sharp point and the sudden jump in frequency from the lower branch to the upper. The lower boundary with its frequencies of 0 to 4 radians per second is practically invariant with servo natural frequency, which indicates that it corresponds to the system mode associated with the airframe short-period oscillatory mode. On the other hand, the upper boundary varies widely with servo natural frequency, which indicates that it is the boundary for another system mode which is associated closely with the control-servo oscillatory mode.

It is interesting to note that a large increase in the stable operating range ( $x/\bar{c} = -0.52$  to  $-1.0$ ) is obtainable by increasing the control-servo natural frequency from 30 to 60 radians per second, while increasing the frequency from 60 to infinity radians per second only results in a small gain in operating range ( $x/\bar{c} = -1.0$  to  $-1.18$ ). Thus, it appears that the servo-natural-frequency requirements for a satisfactory stabilization system of this type would not be particularly severe.

#### Effect of Autopilot Characteristics on the Damping Ratio and Period

Up to this point, only the boundaries of stability have been determined. However, for satisfactory response more than the mere requirement of stability must be specified. In the actual physical

problem the time to damp, time of response and peak overshoot of the transient response resulting from various inputs such as gust disturbances, out-of-trim moments, noise, etc., must be kept within reasonable limits. For example, although the missile-autopilot combination might be stable, if the damping ratio were small, the overshoot in response to a gust might be so large as to cause a large dispersion at burn-out.

Since a quantitative study of the transient response with various inputs is beyond the scope of this report, satisfactory stability will be judged on the basis of "rule of thumb" values of damping ratio for satisfactory stability of a servomechanism. The rule of thumb is that the damping ratio  $\zeta$  be less than 1.0 but greater than 0.35, which corresponds to 0- to 30-percent peak overshoot in the transient response to a step input. For this purpose, the curves of constant damping ratio and period in figures 7 and 8 were constructed by methods mentioned previously in the analysis. Actually two families of damping ratio and period curves exist because there are two oscillatory modes present. However, if the autopilot gearing is restricted to values sufficiently below the upper boundary, as was done in this case, the mode associated with the control servo is well damped and of high enough frequency to be relatively insignificant in the stability problem. For this reason, only the damping ratio and period curves associated with the airframe short-period oscillatory mode are shown. Since these curves are only applicable to autopilots with servo natural frequencies of 60 radians per second or higher, the first-order servo approximation was used in the calculations.

Effect of rate feedback on damping ratio and period.- In figures 7 and 8, a first-order control servo was assumed, and servo time lag and rate-gyro time lag ( $2\zeta_s/\omega_s = 0.03$ ,  $T = 0.02$ ) were held constant while rate was varied. With the rate equal to 0.03 as shown by figure 7, all damping ratios are less than 0.1 below a static margin of -0.03. Hence, it may be seen that although the system is stable at negative static margins, the transient response is so lightly damped that the flight path is apt to be erratic. On the other hand, if the rate is increased to a value of 0.08 as shown by figure 8, large enough damping ratios are available to insure satisfactory stability at negative static margins. Increasing the rate also has the effect of reducing the period which tends to decrease the time of response. Thus the effect of increasing rate is favorable in all respects in improving the transient response to give satisfactory stability.

Although the curves of constant damping ratio and period of figure 8 are shown only to a static margin of -0.06, calculation of the roots of the characteristic stability equation show that damping ratios of greater than 0.35 can be obtained down to a static margin of -0.5. At positive static margins, the damping ratios are much lower and, for this reason,

it would be advantageous to operate the missile entirely in the negative static-margin region.

### Effect of Phugoid and Other Modes on Stability and Transient Response

Stability.- In the analysis and previous discussion only four of the roots of the characteristic stability equation were considered. Because the characteristic stability equation is of higher order than four, other roots with positive real parts might be present. For this reason, the regions within the upper and lower stability boundaries are not indicative of stability unless all the other roots have negative real parts. In order to check these roots and verify the stability of all modes within these stability boundaries, the complete-system characteristic stability equation was formed using three degrees of freedom in the aerodynamic transfer function. From this seventh-order differential equation, another stability boundary was determined which will be called the system phugoid stability boundary. As shown in figure 7, this boundary falls below the  $K = 0$  axis for positive values of static margin, and, in the vicinity of the neutral point, it splits into two aperiodic stability boundaries which fall below the boundaries associated with the short-period and control-servo modes. The three stability boundaries account for six of the roots. The seventh, which may be associated with the time lag in the rate gyro, is a large negative root and is also stable within regions of practical interest. Hence, it may be concluded that the regions within the short-period and control-servo stability boundaries and the  $K = 0$  axis are stable in all modes.

The assumption of two degrees of freedom in the aerodynamics is not valid near the system phugoid stability boundary. However, calculations show that the stability boundaries and curves of constant damping ratio and period are sufficiently accurate down to an autopilot gearing of 0.05 when two degrees of freedom are assumed. The region below this value was not investigated thoroughly because it was out of the practical operating range of autopilot gearings. For this reason the contours of figures 7 and 8 are not shown in the negative region below  $K_1 K_2 = 0.05$ .

Transient response.- In previous discussions, degree of stability was judged by the damping ratio and period of only one mode, the mode associated with the airframe short period. This procedure was used because it was believed that the effect of other modes on the transient response would be insignificant. In order to verify this assumption, the transient response to a step input  $\theta_1$  was determined at a representative number of points by applying Heavisides' Expansion Theorem to the transfer function  $\theta_0/\theta_1$  for three degrees of freedom which gave an



analytical expression for the transient response as a sum of the various modes. From this expression the relative magnitudes of the various modes were determined. It should be remembered that, although the open-loop component modes are interrelated by closing the loop, the principal part of certain modes of the closed-loop system may be attributed to certain of the open-loop component modes. In the following discussion, the roots of the characteristic equation will be identified with the principal open-loop root with which it is associated.

In the stable region of positive autopilot gearing, the characteristic stability equation has two real negative roots which in the region close to the system phugoid boundary are associated with the airframe phugoid. These roots indicate a nonoscillatory subsident motion in the transient response. One of these roots is very small, approximately  $-0.012$ , which means that the time for the motion to reach half amplitude is nearly 60 seconds. Therefore, the time of response (reference 1) would be greatly increased if the maximum value of this subsident motion were large compared to the maximum value of other modes. However, at  $K_d K_g = 0.05$ , which is close to the limit of practical values of autopilot gearing, the maximum value of the subsident motion is only 10 percent of that of the oscillatory mode associated with the airframe short period, and at higher autopilot gearings the percentage is even less. The foregoing indicates that, except near the system phugoid stability boundary, the effect on the transient response of not considering the third degree of freedom is negligible. The other root associated with the phugoid is generally much larger (approximately  $-2$ ) and, hence, the motion damps to half amplitude in 0.35 second. Because it damps rapidly and its amplitude is very small, its contribution to transient response is small. Also, this root is closely associated with  $b_1/a_1$  and occurs to some extent even when two degrees of freedom are assumed.

In the stable region, the characteristic stability equation also has a pair of complex conjugate roots with negative real parts associated with the control-servo mode. As mentioned previously, this mode is of high frequency compared to other modes. However, for values of autopilot gearing well below the upper stability boundary ( $K_d K_g < 1/2$  upper boundary), the maximum amplitude of this mode is less than 1 percent of the mode associated with the missile short period. Hence, except possibly near the upper boundary, the effect of the system servo mode on transient response is negligible.

Another root of the characteristic equation is real, large, and negative, and arises principally from the rate-gyro time-lag term. Since this root is approximately  $-50$ , the motion reaches half amplitude in approximately 0.014 second and, since the maximum value is not excessive, it too may be neglected in the transient response.

## CONCLUDING REMARKS

In this theoretical investigation of the stability of a variable-incidence boost-glide missile with an autopilot, the practicability of obtaining satisfactory stability at negative static margins has been demonstrated. It has been shown that the stable flight region in the autopilot-gearing-static-margin plane is bounded by three stability boundaries, an upper boundary governed principally by the control-servo dynamics, a lower boundary governed principally by the airframe short-period mode, and another lower boundary governed principally by the airframe phugoid mode. With the exception of gearings in close proximity to the system phugoid or the control-servo boundaries, the system mode associated with the airframe short period is the principal mode for gearings on the stable side of the boundaries, and the transient response may be considered as that of a second-order system. Furthermore, curves of constant damping ratio and period for this principal mode may be determined with assumptions of two degrees of freedom for the airframe and a first-order system for the control servo.

Successful operation of this missile-autopilot combination at negative static margin was dependent mainly on two factors: (1) the control-servo natural frequency had to be high enough to permit an adequate range of autopilot gearings, but there appeared to be no particular advantage in going to very high frequencies (higher than 60 radians per second), and (2) the ratio of rate-gyro to displacement-gyro gain  $R$  had to be equal to or greater than the time lag in the control servo ( $2\zeta_s/\omega_s$ ). An increase in time lag tended to decrease the stable region, and an increase in the rate gain tended to increase the stable region up to a rate ratio  $R$  of 0.08. Above this value the range of available autopilot gearings for stability decreases rapidly. With practical values of autopilot settings and reasonable time lags, satisfactory degree of stability is obtained with a variation in static margin from approximately -0.02 to -0.5.

Although these concluding remarks are based on the particular configuration used in the example, it appears that similar results and conclusions would be obtained for a wide class of airplanes and missiles with this type of autopilot, and that satisfactory stable flight at negative static margins is practical even with this simple conventional autopilot.

Ames Aeronautical Laboratory  
National Advisory Committee for Aeronautics  
Moffett Field, Calif.

## REFERENCES


1. Jones, Arthur L., and Briggs, Benjamin R.: A Survey of Stability Analysis Techniques for Automatically Controlled Aircraft. NACA TN 2275, 1951.
  2. Greenberg, Harry: Frequency-Response Method for Determination of Dynamic Stability Characteristics of Airplanes With Automatic Controls. NACA TN 1229, 1947.
  3. Brown, Gordon S., and Campbell, Donald P.: Principles of Servomechanisms. John Wiley and Sons, Inc., N. Y., 1948.
  4. Sternfield, Leonard, and Gates, Ordway B., Jr.: A Method of Calculating a Stability Boundary That Defines a Region of Satisfactory Period-Damping Relationship of the Oscillatory Mode of Motion. NACA TN 1859, 1949.
- 

TABLE I.- STABILITY DERIVATIVES<sup>1</sup> OF  
A SUPERSONIC MISSILE

Mach number . . . . .	2
Altitude, feet . . . . .	30,000
$X_u$ . . . . .	0.0188
$X_\alpha$ . . . . .	$0.0238 - 0.0555 x/\bar{c}$
$X_\theta$ . . . . .	$0.0242 - 0.000385 x/\bar{c}$
$X_\delta$ . . . . .	$0.0568 x/\bar{c}$
$z_u$ . . . . .	0.0159
$z_\alpha$ . . . . .	2.118
$z_\theta$ . . . . .	0
$z_\delta$ . . . . .	1.03
$C_{m_u}$ . . . . .	$0.01311 - 0.0188 x/\bar{c}$
$C_{m_\alpha}$ . . . . .	$-4.18 x/\bar{c}$
$C_{m_{\dot{\alpha}}}$ . . . . .	$-(0.00252 + 0.000223 x/\bar{c})$
$C_{m_{\dot{\theta}}}$ . . . . .	$-(0.01052 + 0.00328 x/\bar{c} + 0.003698 x^2/\bar{c}^2)$
$C_{m_{\dot{\delta}}}$ . . . . .	$1.735 - 2.061 x/\bar{c}$

<sup>1</sup>As expressed in reference 2.

NACA



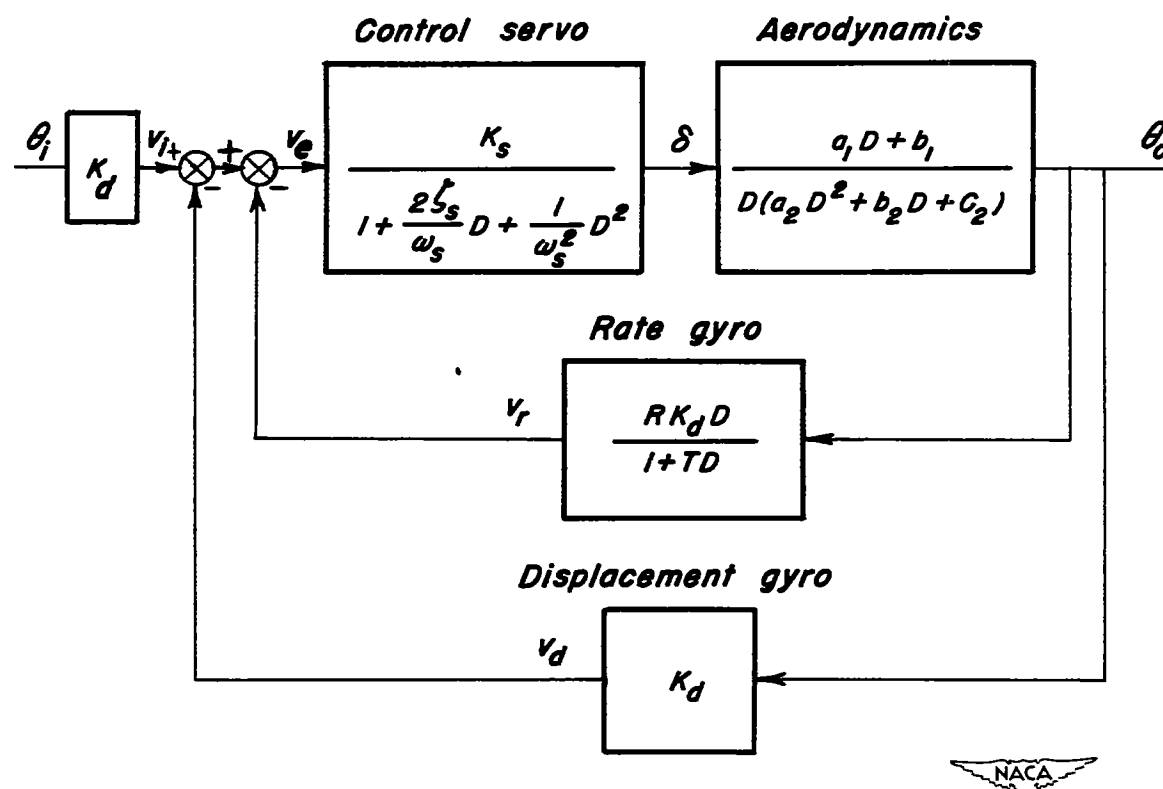
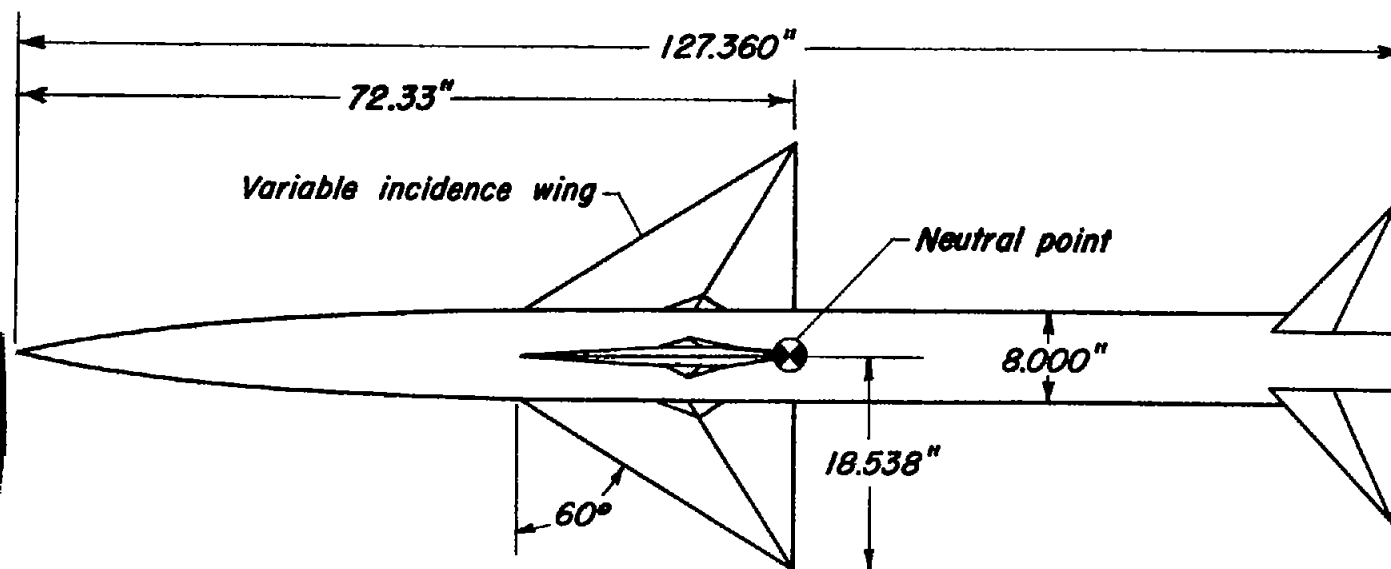


Figure 1.-Block diagram of missile with autopilot.



$S$ , exposed wing area, $\text{ft}^2$	2.531
$\bar{c}$ , mean aerodynamic chord based on $S$ , ft	1.396
$m$ , mass, slugs	6.677
$K_y$ , radius of gyration about principal lateral axis, ft	2.480



Figure 2.—Description of supersonic missile.

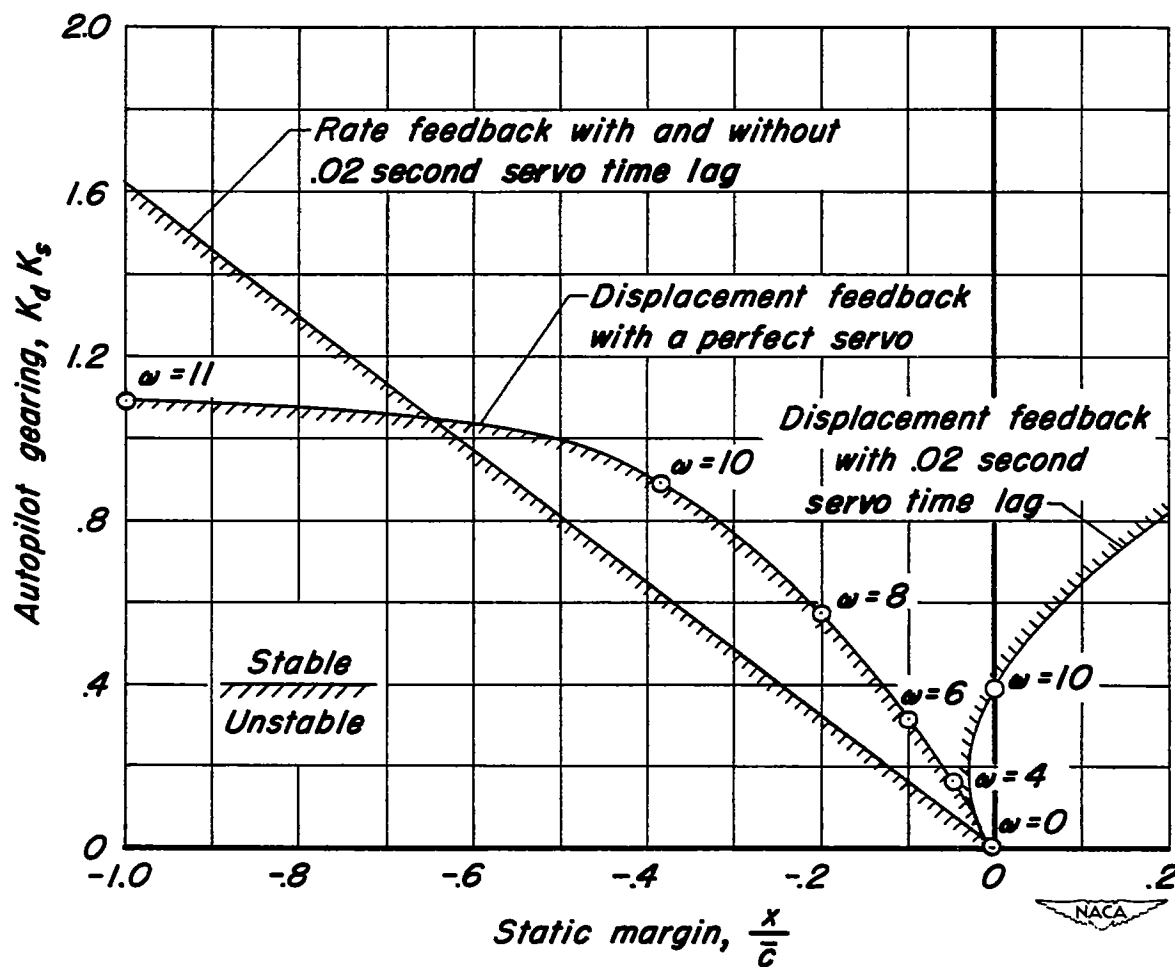


Figure 3.—Stability boundaries of simplified cases.



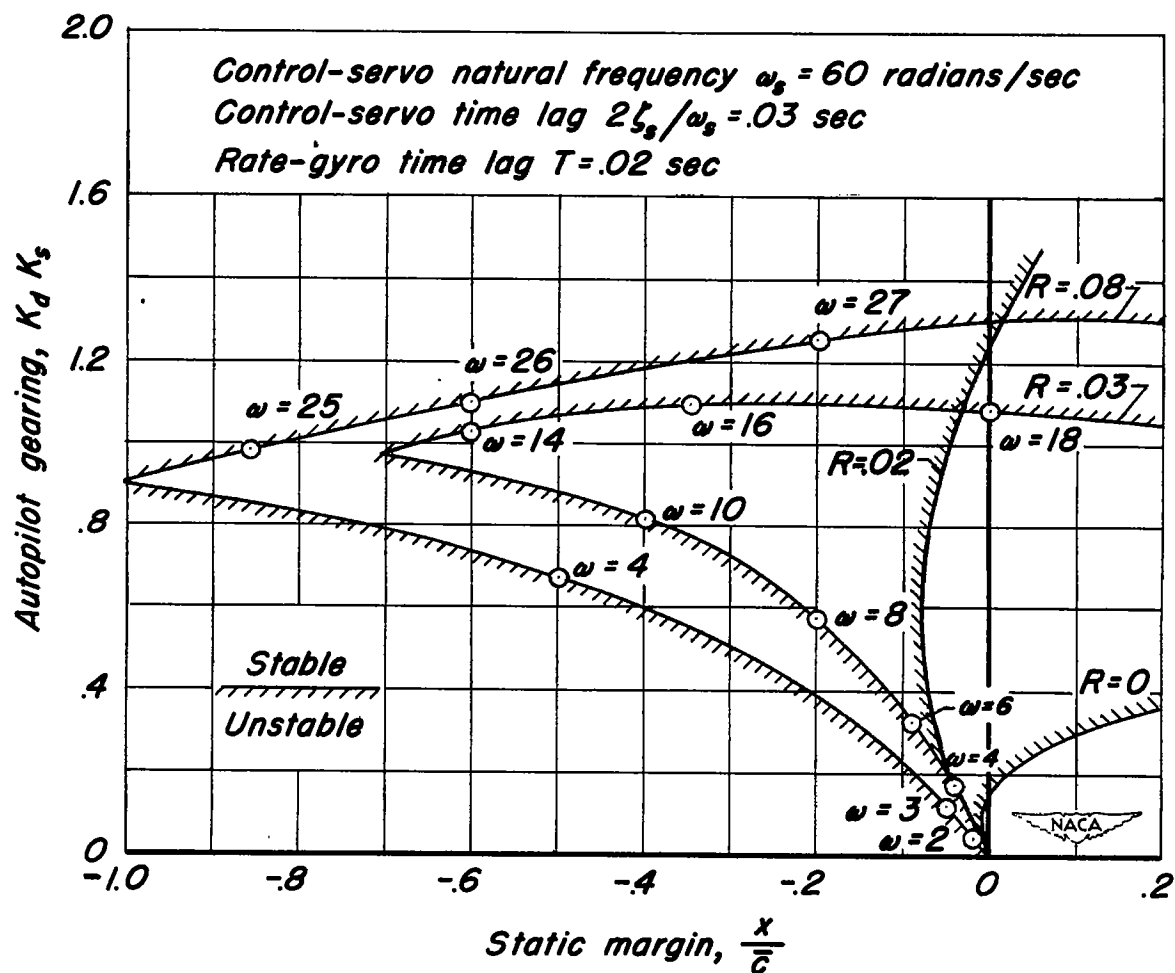


Figure 4.- Effect of rate feedback on stability boundary.

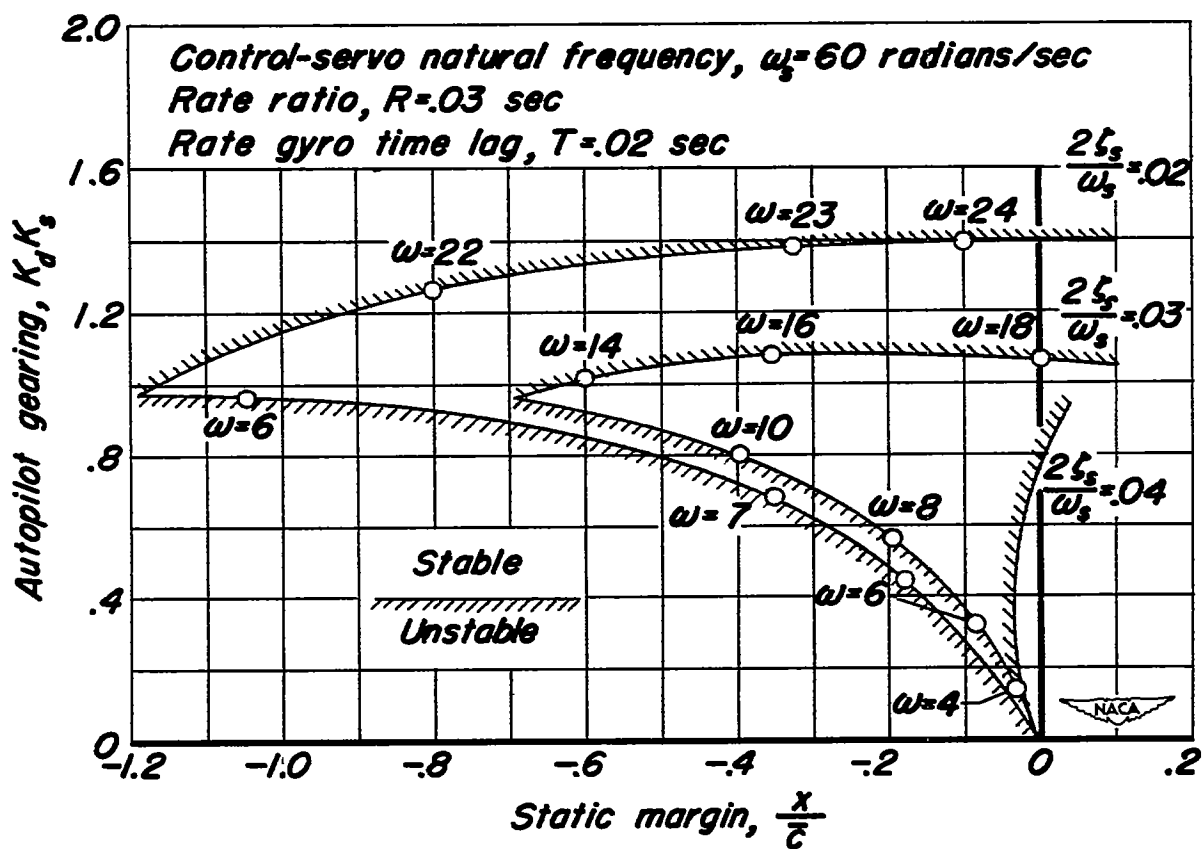


Figure 5.—Effect of control-servo time lag on stability boundaries.

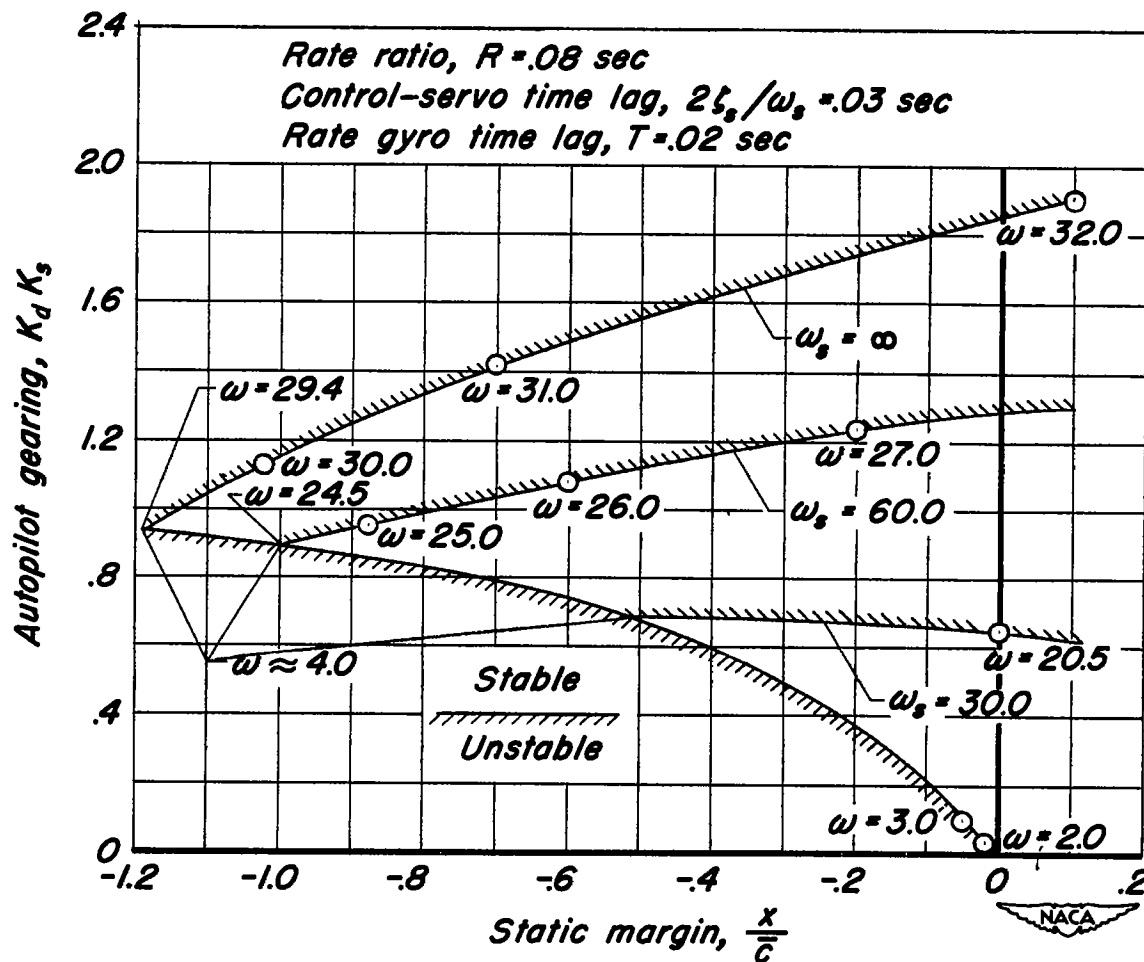


Figure 6.—Effect of control-servo natural frequency on stability boundaries.

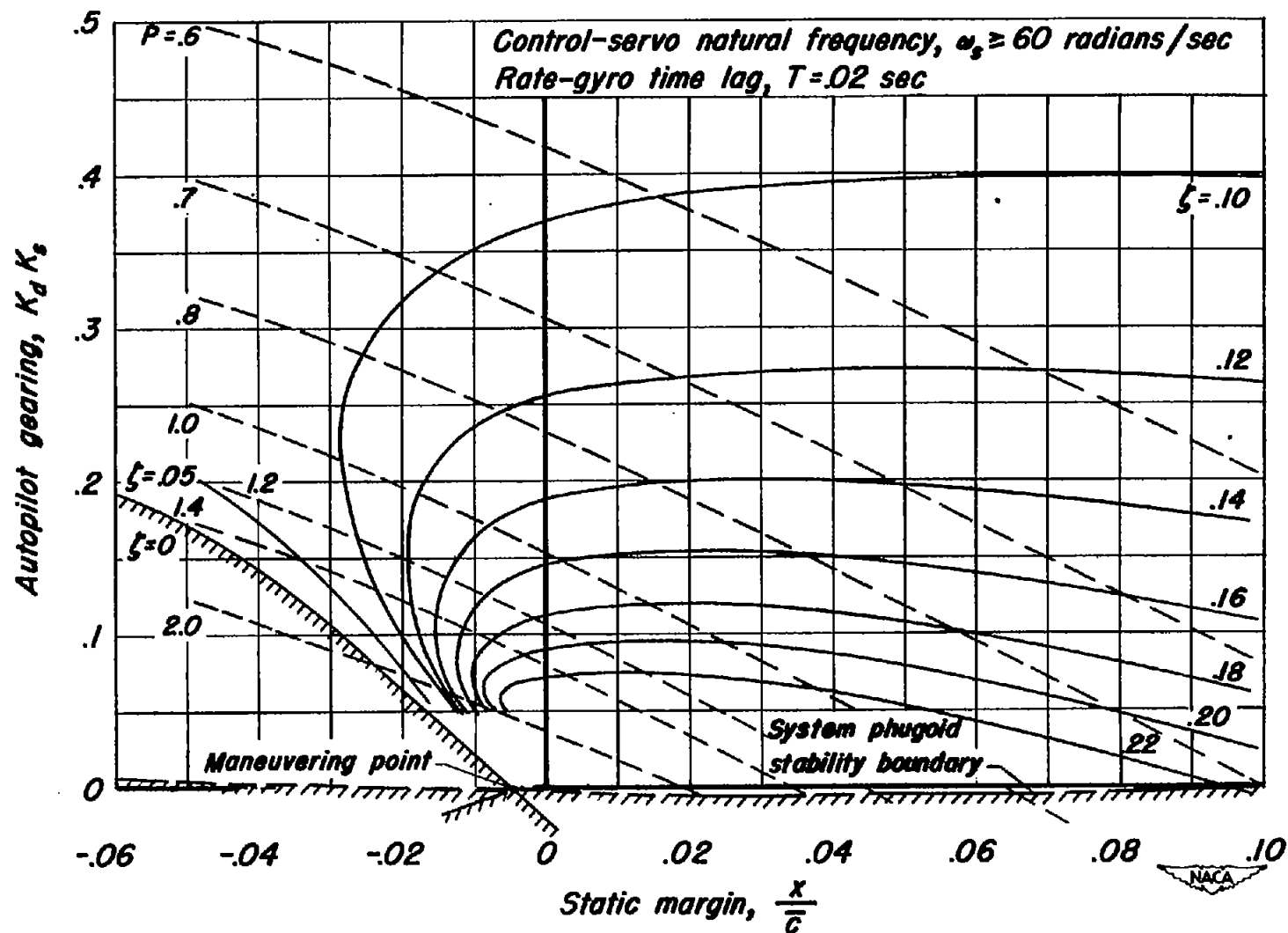


Figure 7.—Period and damping ratio of principal mode for rate ratio equal to control-servo time lag. ( $R = 2\zeta_s/\omega_s = 0.03$  sec).

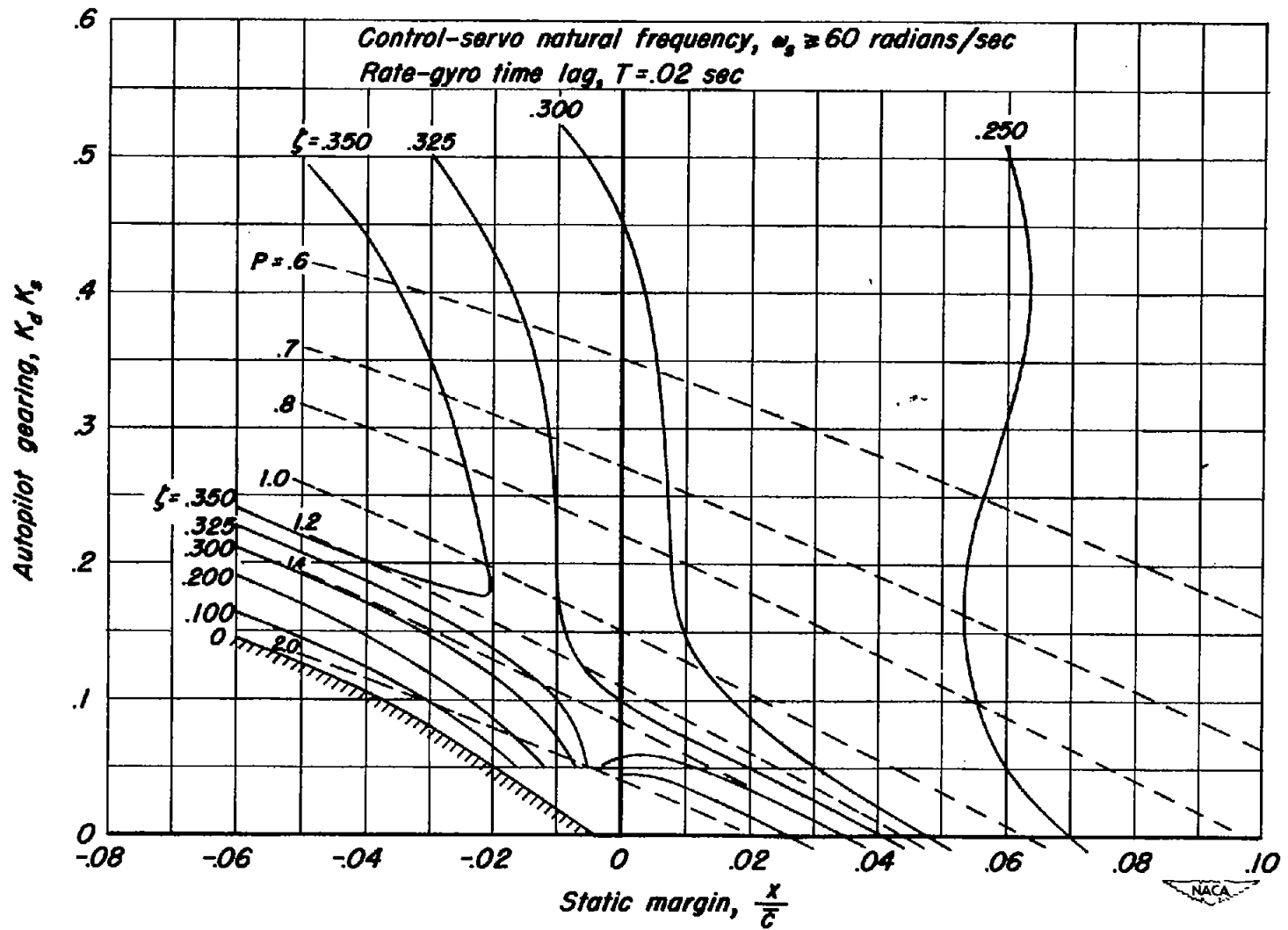


Figure 8.-Period and damping ratio of principal mode for rate ratio greater than control-servo time lag. ( $R \approx .08$  sec,  $2\zeta_s/\omega_s = .03$  sec).